Electroacupuncture in the repair of spinal cord injury: inhibiting the Notch signaling pathway and promoting neural stem cell proliferation

Xin Geng, Tao Sun, Jing-hui Li, Ning Zhao, Yong Wang, Hua-lin Yu[*]

Second Department of Neurosurgery, First Affiliated Hospital of Kunming Medical University, Kunming, Yunnan Province, China

*Correspondence to:
Hua-lin Yu, M.D., yuhualinbio@126.com.

Abstract

Electroacupuncture for the treatment of spinal cord injury has a good clinical curative effect, but the underlying mechanism is unclear. In our experiments, the spinal cord of adult Sprague-Dawley rats was clamped for 60 seconds. *Dazhui* (GV14) and *Mingmen* (GV4) acupoints of rats were subjected to electroacupuncture. Enzyme-linked immunosorbent assay revealed that the expression of serum inflammatory factors was apparently downregulated in rat models of spinal cord injury after electroacupuncture. Hematoxylin-eosin staining and immunohistochemistry results demonstrated that electroacupuncture contributed to the proliferation of neural stem cells in rat injured spinal cord, and suppressed their differentiation into astrocytes. Real-time quantitative PCR and western blot assays showed that electroacupuncture inhibited activation of the Notch signaling pathway induced by spinal cord injury. These findings indicate that electroacupuncture repaired the injured spinal cord by suppressing the Notch signaling pathway and promoting the proliferation of endogenous neural stem cells.

Key Words: nerve regeneration; spinal cord; electroacupuncture therapy; neural stem cells; notch signaling pathway; astrocytes; inflammation; survival curve; proliferation; differentiation; real-time quantitative PCR; western blot assay; neural regeneration

Geng X, Sun T, Li JH, Zhao N, Wang Y, Yu HL (2015) Electroacupuncture in the repair of spinal cord injury: inhibiting the Notch signaling pathway and promoting neural stem cell proliferation. Neural Regen Res 10(3):394-403.

Introduction

There is currently no effective treatment for spinal cord injury (SCI), which results in severe skeletal muscle dystrophy, loss of endurance, loss of fiber cross-sectional area, and loss of force (Dudley-Javoroski and Shields, 2008; Biering-Sorensen et al., 2009; Qin et al., 2010). Furthermore, SCI results in chronic disability, extending the suffering of patients and creating a burden on society. Studies have shown that, after SCI, multiple detrimental factors converge to induce large-scale oligodendrocyte death that results in axonal demyelination of the remaining neurons, which is unfavorable for the recovery of neural function in the damaged spinal cord. Acupuncture is widely used to treat SCI patients (Munce et al., 2013), and improves outcomes after SCI (Gad et al., 2013). Some studies have shown that electroacupuncture (EA) at early and mid-stages of SCI can prevent or inhibit the death of functional neurons (Mekhail et al., 2012). Studies have also shown that treating SCI with EA improves the local microenvironment of the spinal cord, accelerates the reduction of edema, and induces tissue antioxidant formation that lowers the production of excitatory amino acids and inhibits

apoptosis and necrosis (Sun et al., 2010; Ohri et al., 2011; Su et al., 2011). Previous studies have shown that treating SCI with EA induces the repair of neural function (Li et al., 2010; Ding et al., 2011; Huang et al., 2011).

Neural stem cells (NSCs) that form new neurons may improve the function of the damaged nervous system (Arvidsson et al., 2002; Parent et al., 2002).

After SCI, damage to the blood-brain barrier can lead to massive peripheral infiltration of inflammatory cells, and produce large amounts of inflammatory cytokines, which causes progressive degeneration of tissue damage and necrosis (Frei et al., 1990). SCI can also cause cascades at the cellular and molecular levels, and these secondary damage factors can cause serious nerve damage (Choo et al., 2008). Among these secondary injury factors, inflammation is the main one, playing a major role in the pathogenesis of SCI (Trivedi et al., 2006; Donnelly and Popovich, 2008). The Notch signaling pathway is a highly conserved pathway that uses cell-cell interactions to control developmental growth. The Notch signaling pathway is important for cell fate determination, neural system development, organ formation, and

segmentation in vertebrate and invertebrate animal development. Studies have shown that the Notch signaling pathway is involved in repair after SCI (Loy et al., 2002; Fassbender et al., 2011).

In the present study, we investigated the effect of EA on tissue repair after SCI and its underlying mechanisms, providing important insights into the treatment of SCI.

Materials and Methods

Animals
Two-hundred clean adult male Sprague-Dawley rats weighing 300–350 g and aged 6–7 weeks were used for these experiments. Rats were provided by the Experimental Animal Center of Kunming Medical University in China (license No. SCXK (Dian) 2011-0004). All experimental procedures involving animals were carried out in accordance with the US National Institute of Health Guide for the Care and Use of Laboratory Animals and were approved by the Administration Committee of Experimental Animals, Yunnan Province, China.

SCI model and EA stimulation
Sprague-Dawley rats were randomly divided into five groups: control, sham, SCI, sham + EA, and SCI + EA. To provide a range of time points for analysis, animals were sacrificed under anesthesia at 1, 3, 7, 14, 21, 28, and 56 days after injury or sham surgery (or after the start of the experiment in the case of control animals). There were five rats in each time point subgroup. The surgical procedure was performed with animals under general anesthesia. The control group consisted of normal rats without any treatment. In the sham groups, the spinal cords of rats were exposed without surgery. In the SCI groups, the spinal cords of rats were exposed and clamped for 60 seconds according to previous studies (Joshi and Fehlings, 2002; Poon et al., 2007; Rice et al., 2007). In the EA group, the rats were restrained to a board, and two bilateral stainless steel 0.18-mm-diameter needles (Hwato Disposable Acupuncture Needle, Jiangsu Medical Supplies Factory, Jiangsu Province, China) were inserted to a depth of approximately 5 mm at the acupoints corresponding to *Mingmen* (GV4, posterior midline and in the depression below the spinous process of the second lumbar vertebra) and 3 mm at *Dazhui* (GV14, posterior midline and in the depression below the spinous process of the seventh cervical vertebra) and connected to a Hwato SDZ-V electrostimulator (Jiangsu Medical Supplies Factory). EA treatment was administered with 2 Hz stimulation for 30 minutes and the output voltage was set at 2 V. EA was administered once per day. Subjects in the non-EA groups were only restrained for 30 minutes.

Survival and motor function
The survival ratio of rats was calculated using a Kaplan-Meier curve, with $P < 0.05$ in a log-rank test indicating significance. The hindlimb motor function of rats was assessed at 1, 3, 7, 14, 21, 28, and 56 days using the open field locomotor test developed by Basso, Beattie, and Bresnahan (BBB; Basso

et al., 1995). Double independent BBB scores were recorded, and the average values in five rats are presented.

Hematoxylin-eosin staining
Paraffin sections were dewaxed using xylol, stained with hematoxylin (Dingguo, Beijing, China) working solution for 8 minutes, placed in HCl solution (Dingguo) for 5 seconds, washed with running water for 10 minutes, stained with eosin solution (Dingguo) for 5 minutes, and dehydrated in alcohol (Dingguo). The sections were examined under a light microscope (Olympus, Tokyo, Japan).

Enzyme-linked immunosorbent assay (ELISA)
Total blood samples were collected at 1, 3, 7, 14, 21, 28, and 56 days by cutting the tails of rats in each group, and the serum was collected by centrifugation. Tumor necrosis factor-α (TNF-α), interleukin (IL)-1α, IL-6, and IL-10 contents in rats were tested using ELISA kits (Huamei Biological Technology Ltd., Wuhan, China). These assays employed the quantitative sandwich enzyme immunoassay technique. Antibodies specific for TNF-α, IL-1α, IL-6, and IL-10 were pre-coated onto a microplate. The ELISA kits were used according to the manufacturers' instructions and absorbance at a wavelength of 450 nm was detected using a spectrometer plate reader (Bio-Tek company, Vermont, USA) ($n = 5$ rats). After testing, a standard curve was constructed by plotting the mean absorbance for each standard on the *X*-axis against concentration on the *Y*-axis and a best fit line was drawn, determined by regression analysis. Concentrations were calculated from these curves.

Real-time quantitative polymerase chain reaction (qPCR)
Total RNA was isolated from the spinal cords of animals in each group at 1, 3, 7, 14, 21, 28, and 56 days using TRIzol solution (TAKARA Biotechnology Co., Ltd., Dalian, Liaoning Province, China). The expression levels of Notch1, Notch3, Notch4, PS1 and Hes1 genes were measured using a real-time qPCR system (Applied Biosystems, ABI Prism 7300, USA) with SYBR Green (TAKARA Biotechnology Co., Ltd.). cDNA was amplified by PCR using primers for each target gene. The real-time qPCR program was as follows: 95°C for 10 minutes, followed by 35 cycles of 95°C for 15 seconds and 60°C for 31 seconds. The qPCR primer sequences are shown in **Table 1**. The amplification efficiency was compared between the target and reference control (GAPDH) using the delta-delta Ct (ΔΔCt) method (Livak and Schmittgen, 2001).

Western blot assay
All spinal cord tissues (T_{10} spinous process) obtained at 1, 3, 7, 14, 21, 28, and 56 days in each group were homogenized in lysis buffer (Kangwei Biotechnology, Beijing, China). Equal amounts of proteins were separated by sodium dodecyl sulfate-polyacrylamide gel electrophoresis, and then the resolved proteins were transferred to a nitrocellulose membrane (Whatman, Dassel, Germany). The membrane was incubated with primary antibodies overnight at 4°C. The primary antibodies used were: mouse monoclonal IgG

Notch1 (A-8) (1:1,000; Santa Cruz Biotechnology, Santa Cruz, CA, USA); rabbit polyclonal Notch3 (M-134) (1:1,000; Santa Cruz Biotechnology); goat polyclonal IgG Notch4 (L-16) (1:1,000; Santa Cruz Biotechnology); goat polyclonal IgG PS1 (C-20) (1:1,000; Santa Cruz Biotechnology); and rabbit polyclonal IgG Hes1 (H-140) (1,000; Santa Cruz Biotechnology). Subsequently, the membranes were incubated with secondary antibody at room temperature for 2 hours. β-Actin antibody (1:2,000; Santa Cruz Biotechnology) was used as a loading control for all experiments. The immunoreactive bands were visualized using an enhanced chemiluminescence reagent (Beyotime, Beijing, China). The grayscale values of bands were quantified using Image J software (Fujifilm, Tokyo, Japan). The relative expression of protein was calculated based on the ratio of target grayscale values to loading control grayscale values.

Immunohistochemistry

The injured spinal cords were removed at 1, 3, 7, 14, 21, 28, and 56 days in each group and post-fixed overnight in paraformaldehyde. Serial sections (4-μm thickness) were cut from a paraffin block. The following primary antibodies were used: mouse monoclonal antibody nestin (Rat-401) (dilution 1:100); and rabbit polyclonal antibody glial fibrillary acidic protein (GFAP) (H-50) (1:100) (Santa Cruz Biotechnology). The sections were incubated with primary antibody overnight at 4°C, and then incubated with horseradish peroxidase-conjugated goat anti-mouse secondary antibody (1:500) and goat anti-rabbit secondary antibody (1:500) (Santa Cruz Biotechnology) for 2 hours at room temperature. The reactions were visualized using 3,3′-diaminobenzidine reagent (Boster Biological Technology Ltd., Wuhan, Hubei Province, China). Nuclei were counterstained with hematoxylin. The sections were examined under a light microscope (Olympus, Tokyo, Japan). Brown staining indicated immunoreactive cells and blue staining indicated nuclei. Three representative staining fields for nestin and GFAP of each section were analyzed to produce a mean optical density value using Image-Pro Plus 6.0 software (Media Cybernetics Inc., USA), which represents the strength of staining signals as measured per positive pixel.

Statistical analysis

All data are expressed as the mean ± SD. Data were analyzed by one-way analysis of variance and Tukey's *post hoc* test using GraphPad Prism Version 5.0a software (GraphPad Software Inc., CA, USA). A value of $P < 0.05$ was considered statistically significant.

Results

Effects of EA on survival ratios and behavior in rats with SCI

Survival, weight, and behavioral scores for each group of rats are shown in **Figure 1A–C**. As shown in the survival curves, compared with the control group, the survival ratio was significantly lower in the SCI group ($P < 0.001$). The survival ratio was also lower in the SCI + EA group than in the con-

trol group ($P < 0.01$); however, it was significantly higher in the SCI + EA group than in the SCI group ($P < 0.05$). BBB score was significantly lower in the SCI group and SCI + EA group (both $P < 0.05$) than in the control group. BBB score was significantly higher in the SCI + EA group than in the SCI group ($P < 0.05$). After treatment with EA, rats conditions improved in each group (both $P < 0.05$). The results in the sham group and the sham + EA group suggest that EA did not have any side effects in normal rats.

EA promoted morphological recovery in rats with SCI

Results from hematoxylin-eosin staining of spinal cords showed that rat spinal sections from animals in the control, sham and sham + EA groups displayed normal gray and white matter; the anterior horn neurons had large round nuclei with clear large nucleoli, and the structure of the central canal was clear without hemorrhagic necrosis, edema, or degeneration. After SCI, the injured region showed disruption of structure, blurred visualization, bleeding in the central canal, multifocal hemorrhage in the gray matter, and sporadic localized hemorrhage in the white matter. Furthermore, anterior horn neurons in the gray matter displayed pyknosis of nuclei. In the SCI group, at 1 day after SCI, there were structural disruptions in the central canal, edema in the white matter, and traces of hemorrhage. At 3 days after SCI, there was edema in the gray and white matter around the area of central damage. There was structural disruption of the gray and white matter with substantial hemorrhage of the white matter at the affected region. The structures of spinal cord neurons were disrupted, and empty vacuoles were visible between the gray and white matter in the damaged region. In addition, the neurons were swollen, pyknosis of part of the neuronal nuclei was observed, and the boundary for the gray matter in the spinal cord was blurred. At 7 days, the structure of the gray and white matter was disorganized with unclear boundaries, the gray matter lamina was lost, and empty vacuoles remained visible between the gray and white matter in the damaged region. At 14 days, the gray and white matter boundary was still blurred with no hemorrhage, and there were visible empty vacuoles between the gray and white matter. At 21 days, a subtle gray and white matter boundary was visible, and neuronal edema was alleviated. However, the empty vacuoles remained visible at the site of SCI. At 28 days, abnormalities of the white matter were gradually restored, and a clear gray and white matter boundary appeared with the presence of empty vacuoles. At 56 days, swelling and small vacuoles were slightly visible with a clear gray and white matter boundary. Compared with the seven time points in the SCI group, the SCI + EA group rats showed similar trends. However, with EA treatment, the level of SCI was not as severe as in the SCI group, with no display of large-scale edema or empty vacuoles and improved tissue repair and recovery compared with that in the SCI group (**Figure 1D**). These results show that EA provided a reparative effect on SCI rats.

EA inhibited the content of proinflammatory cytokines in the serum of SCI rats

SCI pathology involves an inflammatory response, and

excessive inflammation damages normal tissue and inhibits functional recovery after SCI. Key factors that play important roles in secondary damage are proinflammatory cytokines, including IL-1, IL-6, and TNF-α (Pineau and Lacroix, 2007). Rats in the control group, sham group, and sham + EA group showed no changes in TNF-α, IL-1a, IL-6, IL-10, whereas rats in the SCI group and SCI + EA group showed gradually increased expression of proinflammatory cytokines at 1 day after surgery ($P < 0.001$), reaching the highest expression level at 3 days ($P < 0.01$). Proinflammatory cytokine expression started decreasing at 7 days ($P < 0.001$) and stabilized at 28 days ($P < 0.01$). However, rats in the SCI group displayed higher expression than did those in the SCI + EA group at each time point ($P < 0.05$; **Figure 2**). This result indicates that SCI-induced inflammation and EA treatment inhibited the expression of TNF-α, IL-1a, IL-6 and IL-10 to induce tissue repair in SCI rats.

EA suppressed Notch signaling pathway-related factors in injured spinal cords of rats

To analyze the mechanism by which EA mediates repair after SCI, we used real-time qPCR and western blot assays to study the relationship between EA and Notch-related factors. We found that, at each time point, the expression of Notch1, Notch3, Notch4, PS1, and Hes1 mRNA among the control, sham, and sham + EA groups was not significantly altered, whereas the expression levels were significantly increased in the SCI group and SCI + EA group, peaking at 14 days and decreasing afterwards. However, rats in the SCI + EA group displayed a decreasing trend compared with those in the SCI group, although compared with the control, sham, and sham + EA groups, they still displayed a significant increase (**Figure 3**; $P < 0.001$ or $P < 0.01$ or $P < 0.05$). These results primarily showed that SCI activated the Notch signaling pathway and EA inhibited this SCI-activated Notch signaling pathway ($P < 0.05$). Similarly, we analyzed the levels of Notch signaling pathway-related factors. Western blot assay results showed the same trend as did the qPCR assay (**Figure 4**). The above results showed that the Notch signaling pathway was activated rapidly after SCI and inhibited after EA treatment.

EA improved the proliferation of neural stem cells (NSCs) and inhibited NSC differentiation into astrocytes

Immunohistochemical results revealed that the effects of EA treatment after SCI in rats were mediated by inhibiting astrocyte expression and inducing NSC differentiation.

As shown in **Figure 5A**, GFAP-immunoreactive cells contained brown yellow spots or particles. Compared with the control group, sham group, and sham + EA group, the number of GFAP-immunoreactive cells was increased in the SCI group at 1 ($P < 0.01$), 3 ($P < 0.01$), 7 ($P < 0.001$) and 14 days ($P < 0.001$). The number of GFAP-immunoreactive cells in the SCI group peaked at 14 days and then stabilized without continued increases at 21 days ($P < 0.01$). Compared with the SCI group, a significant inhibition of this increase in the number of GFAP-immunoreactive cells was visible with time in the SCI + EA group. However, the number of immunore-active cells was still higher in the SCI + EA group than in the control, sham, and sham + EA groups at 1 ($P < 0.05$), 3 ($P < 0.01$), 7 ($P < 0.01$) and 14 ($P < 0.01$), 21 ($P < 0.01$), 28 ($P < 0.01$), and 56 days ($P < 0.01$). At 28 days, no further inhibition of the increase in the number of GFAP-immunoreactive cells was seen in the SCI + EA group and the level of immunoreactivity stabilized ($P < 0.01$). However, the number of GFAP-immunoreactive cells in the SCI + EA group was always lower than that in the SCI group and higher than those in the control, sham, and sham + EA groups ($P < 0.05$). Nestin-immunoreactive cells showed nestin cytoplasmic staining, and the cells showed ovoid or triangular protrusions. The control, sham, and sham + EA groups displayed more nestin-immunoreactive cells and these immunoreactive cells were denser. Compared with the control, sham, and sham + EA groups, nestin-immunoreactive cells were rare in the SCI group, and were significantly decreased in number, with a gradually decreasing trend at 1 day ($P < 0.05$). However, the nestin-immunoreactive cell bodies were larger, with large, long protrusions, and showed time-dependent increase in body size in the SCI + EA group ($P < 0.05$; **Figure 5B**). We also quantified the mean optical density of these proteins, as shown in **Figure 5C**. These results showed that, after SCI, expression of nestin protein was suppressed. The proliferation and differentiation of NSCs were significantly increased with EA treatment and peaked at 14 days ($P < 0.05$), although the levels of proliferation and differentiation were still lower than those in the control groups. These results also showed that 2 weeks after SCI was the optimal time for repair.

Discussion

We found that EA decreased the levels of inflammatory factors (TNF-α, IL-1a, IL-6 and IL-10), inhibited the activation of the Notch signaling pathway and GFAP protein expression, subsequently promoted the proliferation of neural stem cells, and repaired the spinal cord following SCI. SCI is the pathophysiological process of SCI-induced neural damage, including the initial mechanical disruption or primary injury, followed by a series of cellular and molecular events that result in secondary damage or secondary injury (Park et al., 2004). Secondary injury includes edema, ion toxicity, free radical formation, fatty acid oxidation, and inflammation, which can result in necrosis, apoptosis, neuronal demyelination, and axonal degeneration. The results of ELISA showed that EA obviously suppressed the inflammatory reaction.

Modern Chinese medicine analyzes the location of injury and the physiological function of EA, and considers the mechanism of action of EA in treating SCI. With the deepening of our knowledge of electrical stimulation-induced regeneration, EA treatment has been used to treat SCI, and clinical and experimental results have shown the efficacy of EA and electric field therapy for SCI (Loy et al., 2002; Conboy et al., 2003; Benedito et al., 2009; Fassbender et al., 2011). However, the detailed mechanisms underlying its effects are not clear. In the present study, we investigated the detailed mechanisms underlying EA treatment.
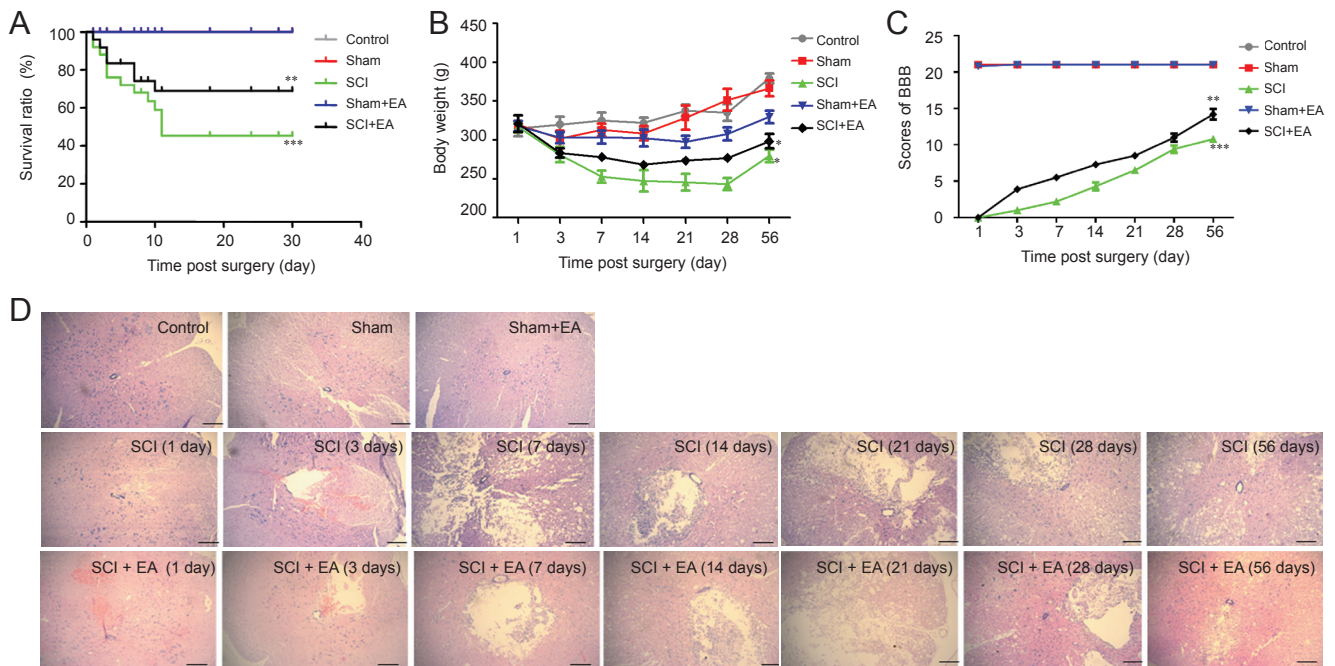
Figure 1 EA treatment in the repair of SCI.
(A) Survival curves for rats. The percentage of rats surviving over time is shown. The survival ratios in the control, sham and sham + EA groups are 100%. The survival ratio was approximately 45.33% in the SCI group, and 68.90% in the SCI + EA group. (B) Body weight changes from 1 to 56 days of rats. The weights of surviving mice over time are shown. (C) BBB scores in rats, recorded at 1, 3, 7, 14, 21, 28 and 56 days. *$P < 0.05$, **$P < 0.01$, ***$P < 0.001$, *vs.* control group. (A–C) Data are expressed as the mean ± SD ($n = 5$; one-way analysis variance and Tukey's *post hoc* test). (D) Hematoxylin-eosin staining: histological changes in the spinal cords of rats (× 200). Scale bars: 100 μm. Spinal cords had similar appearances at different time points in the control, sham and sham + EA groups. There was a progressive enlargement of the cavity in the SCI group, occurring in a time-dependent manner, and a significant recovery in the SCI + EA group. SCI: Spinal cord injury; EA: electroacupuncture; BBB: Basso, Beattie, and Bresnahan.

Table 1 Primer sequences for real-time PCR

Gene	Sequences (5′–3′)	Product size (bp)
Nocth1	Forward: CCT TTA CCT GCC TCT GCC	150
	Reverse: GTC CTG TGG TCC CCT TGA	
Nocth3	Forward: TGT AGT GAT GCT GGA GAT TGA	141
	Reverse: CGT AGT GGG TAT GGG AAA T	
Nocth4	Forward: TCC TCC TAT TTC TGT CGC TG	170
	Reverse: ACT TTT GAG CAG TTC TGT CCT T	
Hes1	Forward: GAG GCT GCC AAG GTT TTT	189
	Reverse: GGT GGG CTA GGG AGT TTA TG	
ps1	Forward: GCT CAA AAG TAC ACG ACG CT	99
	Reverse: TGT GAA AGA ATG GCA GGA	
GAPDH	Forward: ACG GCA AGT TCA ACG GCA CAG	146
	Reverse: GAC GCC AGT AGA CTC CAC GAC A	

GAPDH: Glyceraldehyde-3-phosphate dehydrogenase.

NSCs are a type of cells with self-replication and pluripotent capabilities. NSCs can replace various types of dead cells in the injured spinal cord, making them an ideal and clinically valuable type of cells. These cells differentiate into the various cells of the neural system after proliferation. Since 1992, when the presence of NSCs was first discovered in the corpus striatum (Gage, 2000), considerable research has confirmed the prevalence of NSCs in the central nervous system, including in the spinal cord (Morshead et al., 1994; Chillakuri et al., 2012). NSCs possess the ability to divide, proliferate, regenerate, and differentiate into all of the neural cells of the central nervous system, including neurons, astrocytes, and oligodendrocytes (Suh et al., 2007; Zhao et al., 2008). Their discovery reversed the original conception that neural regeneration was not possible after central nervous system injury and provided new hope for the restoration of neural function after central nervous system injuries, such as SCI. In addition, the use of NSCs as seed cells for central nervous system repair has become a basic and popular aspect of neuroscience research. The discovery of this mechanism has provided novel insights into potential targeted clinical treatment of SCI. Nestin is expressed during the development and differentiation of neural stem cells. Nestin is regarded as a marker for NSCs or neural precursor cells during central nervous system development (Almazan et al., 2001). GFAP is a primary component of astrocytes, is used in the construction of the astrocyte cytoskeleton, and is involved in locomotion and morphology regulation (Casper and McCarthy, 2006). Under SCI conditions, neural stem cell differentiation is limited, especially under the influence of astrocytes and oligodendrocytes. Based on the results of immunohistochemistry for nestin and GFAP proteins, it is implied that EA induces the proliferation of NSCs and inhibits NSC differentiation into astrocytes and oligodendroglias (not
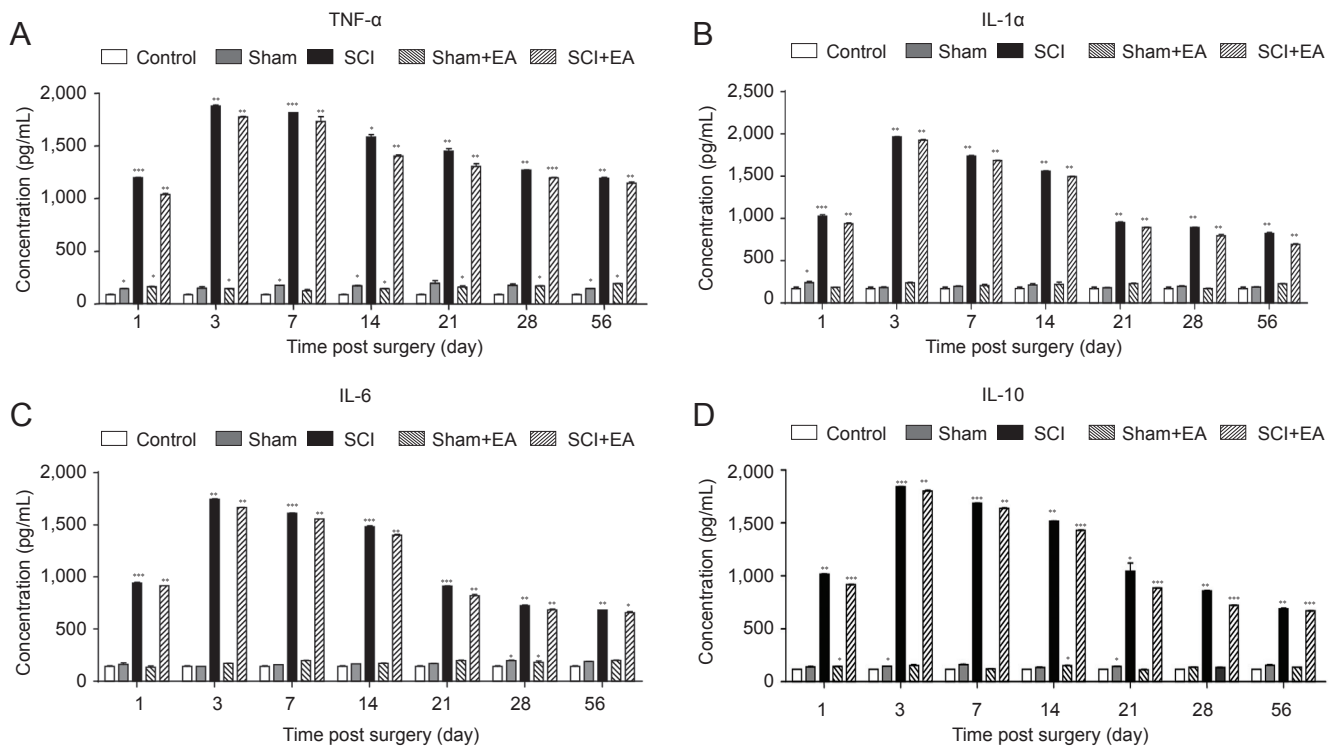
**Figure 2 Effect of EA on serum concentrations of inflammatory cytokines in SCI rats.**
Serum concentrations of TNF-α (A), IL-1α (B), IL-6 (C) and IL-10 (D) inflammatory cytokines were detected by ELISA. Standard curves were constructed by plotting the mean absorbance for each standard on the X-axis against the concentration on the Y-axis and a best fit line was drawn, determined by regression analysis. *$P < 0.05$, **$P < 0.01$, ***$P < 0.001$, *vs.* control group. Data are expressed as the mean ± SD ($n = 3$; one-way analysis of variance and Tukey's *post hoc* test). The experiment was repeated in triplicate. SCI: Spinal cord injury; TNF: tumor necrosis factor; IL: interleukin; EA: electroacupuncture; ELISA: enzyme-linked immunosorbent assay.

shown in this paper).

During nervous system development, the Notch signaling pathway induces many long-term effects on neighboring cells, including neurons and neuroglia (Louvi and Artavanis-Tsakonas, 2006). The Notch signaling pathway is important for cell fate determination, neural system development, organ formation, and segmentation in vertebrate and invertebrate animal development. Notch is a highly conserved receptor protein that is expressed ubiquitously on the cellular membrane and involved in intercellular signaling pathways. In adult mammals, the Notch signaling pathway is essential in vascular development and maintenance (Liu et al., 2003; Karsan, 2005). Notch modulates many proteins, and mutations of Notch or its corresponding ligands results in numerous diseases (Conboy et al., 2003). Studies have shown that the Notch signaling pathway is involved in repair after SCI (Loy et al., 2002; Fassbender et al., 2011). Pathological obstruction of the central nervous system vasculature, such as that caused by ischemic stroke or SCI, compromises the integrity of neural tissue. Although angiogenesis occurs at 3–14 days after SCI, normal vascular markers are absent in most capillaries (Benton et al., 2008; Benedito et al., 2009). The Notch signaling pathway may be an effective pathway regulating the recovery of vascular formation and capillary functional morphology. Our findings in the present study suggest that the Notch signaling pathway induces

NSCs to differentiate into glial cells, which is not beneficial to treating SCI, and inhibits NSC proliferation. The Notch signaling pathway plays an important part in environment-dependent cell fate specification during neurodevelopment. Therefore, research into the relationship between EA treatment and the Notch signaling pathway in SCI is both promising and significant. With the constant advancement of regenerative medicine, EA treatment and signal transduction, this knowledge will have a positive impact on future clinical treatment.

Importantly, we investigated the mechanism underlying the effects of EA on SCI at the molecular level. Our experiments used detailed and accurate groups and time points; the results in the sham + EA group implied that EA treatment had no side effects, and the detailed time points provided evidence for the best time for repair of SCI. The results show that EA treatment of SCI inhibits the Notch signaling pathway and proinflammatory cytokine expression, induces NSC proliferation and differentiation, and inhibits the differentiation of NSCs into astrocytes, thereby inducing morphological recovery from SCI. In conclusion, the repair processes induced by EA after SCI are mediated by inhibiting the Notch signaling pathway and inducing NSC proliferation. These findings provide evidence for the widespread clinical utilization of EA. However, there are some deficiencies in this study, and additional studies are
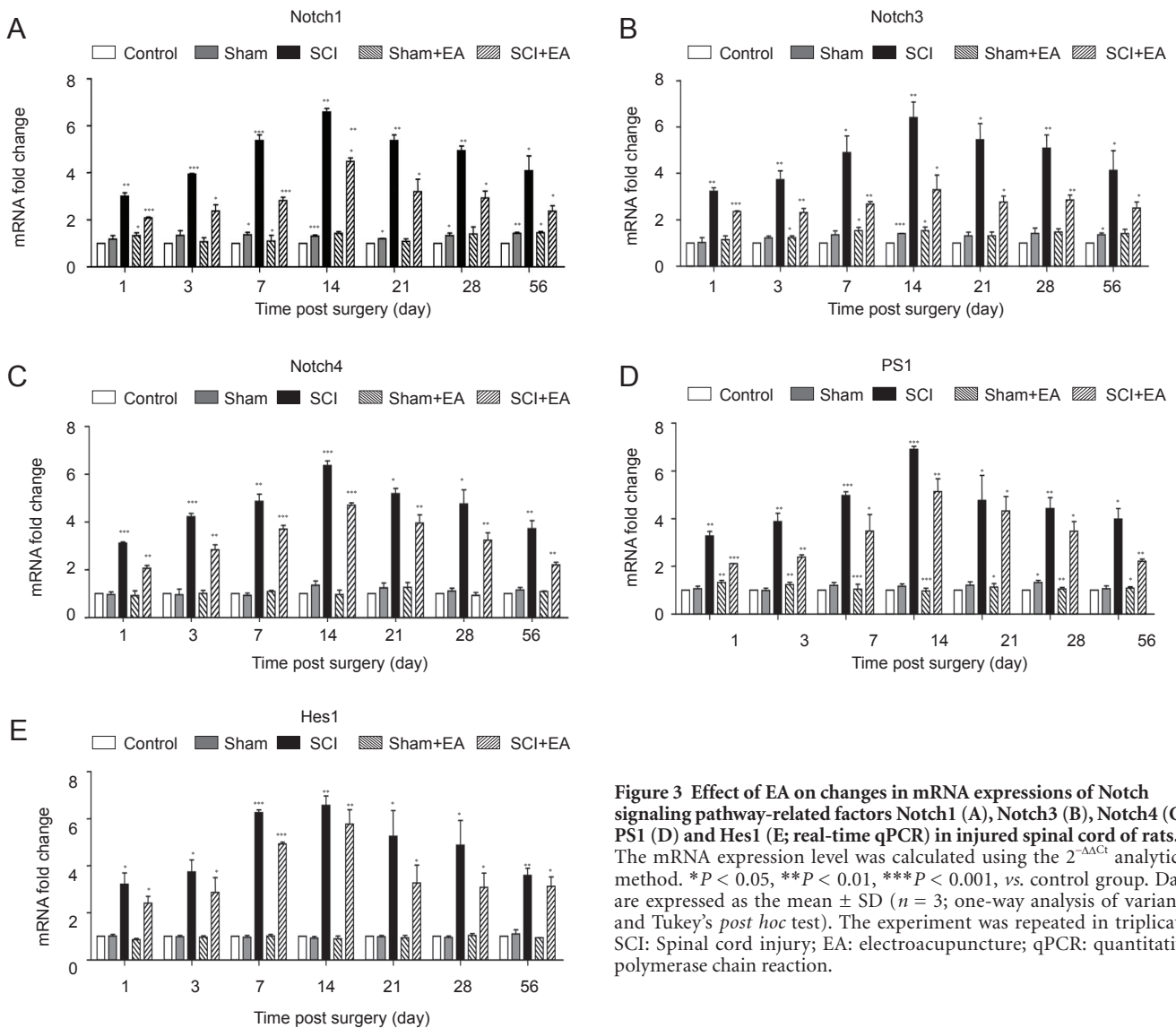
Figure 3 Effect of EA on changes in mRNA expressions of Notch signaling pathway-related factors Notch1 (A), Notch3 (B), Notch4 (C), PS1 (D) and Hes1 (E; real-time qPCR) in injured spinal cord of rats.
The mRNA expression level was calculated using the $2^{-\Delta\Delta Ct}$ analytical method. $*P < 0.05$, $**P < 0.01$, $***P < 0.001$, *vs.* control group. Data are expressed as the mean $\pm$ SD ($n = 3$; one-way analysis of variance and Tukey's *post hoc* test). The experiment was repeated in triplicate. SCI: Spinal cord injury; EA: electroacupuncture; qPCR: quantitative polymerase chain reaction.

necessary emplying methods such as RNA interference and electrophysiology techniques.

Conflicts of interest: *None declared.*

References

Almazan G, Vela JM, Molina-Holgado E, Guaza C (2001) Re-evaluation of nestin as a marker of oligodendrocyte lineage cells. Microsc Res Tech 52:753-765.

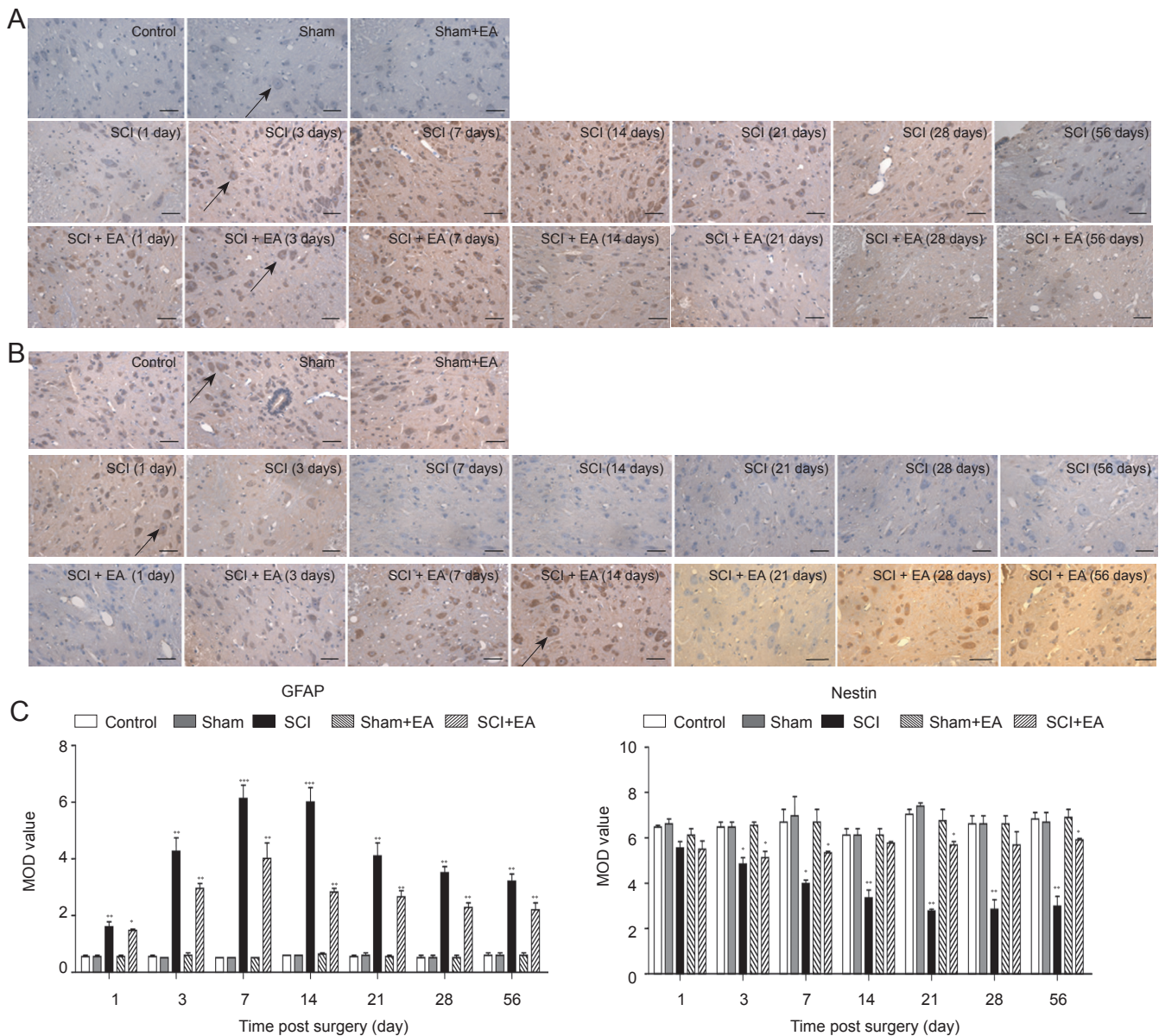Arvidsson A, Collin T, Kirik D, Kokaia Z, Lindvall O (2002) Neuronal replacement from endogenous precursors in the adult brain after stroke. Nat Med 8:963-970.

Basso DM, Beattie MS, Bresnahan JC (1995) A sensitive and reliable locomotor rating scale for open field testing in rats. J Neurotrauma 12:1-21.

Benedito R, Roca C, Sorensen I, Adams S, Gossler A, Fruttiger M, Adams RH (2009) The notch ligands Dll4 and Jagged1 have opposing effects on angiogenesis. Cell 137:1124-1135.

Benton RL, Maddie MA, Minnillo DR, Hagg T, Whittemore SR (2008) Griffonia simplicifolia isolectin B4 identifies a specific subpopulation of angiogenic blood vessels following contusive spinal cord injury in the adult mouse. J Comp Neurol 507:1031-1052.

Biering-Sorensen B, Kristensen IB, Kjaer M, Biering-Sorensen F (2009) Muscle after spinal cord injury. Muscle Nerve 40:499-519.

Casper KB, McCarthy KD (2006) GFAP-positive progenitor cells produce neurons and oligodendrocytes throughout the CNS. Mol Cell Neurosci 31:676-684.

Chillakuri CR, Sheppard D, Lea SM, Handford PA (2012) Notch receptor-ligand binding and activation: insights from molecular studies. Semin Cell Dev Biol 23:421-428.

Choo AM, Liu J, Dvorak M, Tetzlaff W, Oxland TR (2008) Secondary pathology following contusion, dislocation, and distraction spinal cord injuries. Exp Neurol 212:490-506.

Conboy IM, Conboy MJ, Smythe GM, Rando TA (2003) Notch-mediated restoration of regenerative potential to aged muscle. Science 302:1575-1577.

Figure 4 Effect of EA on changes in protein expressions of Notch signaling pathway-related factors Notch1, Notch3, Notch4, PS1 and Hes1.

(A) Western blotting bands for Notch1, Notch3, Notch4, PS1 and Hes1 in different groups. (B) Quantification of protein expression of Notch1, Notch3, Notch4, PS1 and Hes1. *Y*-axis indicates the relative optical density of protein bands (the ratio of target grayscale values to loading control grayscale values). *$P < 0.05$, **$P < 0.01$, ***$P < 0.001$, *vs.* control group. Data are expressed as the mean ± SD ($n = 3$; one-way analysis of variance and Tukey's *post hoc* test). The experiment was repeated in triplicate. SCI: Spinal cord injury; EA: electroacupuncture; d: day(s).

Figure 5 EA effects on NSC proliferation in rats after SCI.
(A, B) Immunohistochemical staining for GFAP (A) and nestin (B) separately in the spinal cord. The reactions were visualized using 3,3′-diaminobenzidine tetrahydrochloride reagent, and the nuclei were counterstained with hematoxylin ($\times$ 400). Scale bars: 50 μm. GFAP-immunoreactive cells contain brown spots or particles. The nestin-immunoreactive cells showed cytoplasmic staining, and the cells showed ovoid or triangular protrusions. Arrows indicate the GFAP- and nestin-immunoreactive cells. (C) Quantification of nestin- and GFAP-immunoreactive cells. Fewer GFAP-immunoreactive cells were seen in the SCI + EA group than in the SCI group. Higher numbers of nestin-immunoreactive cells were seen in the SCI + EA group than in the SCI group ($*P < 0.05$, $**P < 0.01$, $**P < 0.001$). Data are expressed as the mean ± SD ($n = 3$; one-way analysis of variance and Tukey's *post hoc* test). The experiment was repeated in triplicate. SCI: Spinal cord injury; EA: electroacupuncture; GFAP: glial fibrillary acidic protein; NSC: neural stem cell; MOD: mean optical dentsity.

Ding Y, Yan Q, Ruan JW, Zhang YQ, Li WJ, Zeng X, Huang SF, Zhang YJ, Wang S, Dong H, Zeng YS (2011) Bone marrow mesenchymal stem cells and electroacupuncture downregulate the inhibitor molecules and promote the axonal regeneration in the transected spinal cord of rats. Cell Transplant 20:475-491.

Donnelly DJ, Popovich PG (2008) Inflammation and its role in neuro-protection, axonal regeneration and functional recovery after spinal cord injury. Exp Neurol 209:378-388.

Dudley-Javoroski S, Shields RK (2008) Muscle and bone plasticity after spinal cord injury: review of adaptations to disuse and to electrical muscle stimulation. J Rehabil Res Dev 45:283-296.

Fassbender JM, Myers SA, Whittemore SR (2011) Activating Notch signaling post-SCI modulates angiogenesis in penumbral vascular beds but does not improve hindlimb locomotor recovery. Exp Neurol 227:302-313.

Frei K, Nadal D, Fontana A (1990) Intracerebral synthesis of tumor necrosis factor-alpha and interleukin-6 in infectious meningitis. Ann N Y Acad Sci 594:326-335.

Gad P, Choe J, Nandra MS, Zhong H, Roy RR, Tai YC, Edgerton VR (2013) Development of a multi-electrode array for spinal cord epidural stimulation to facilitate stepping and standing after a complete spinal cord injury in adult rats. J Neuroeng Rehabil 10:2.

Gage FH (2000) Mammalian neural stem cells. Science 287:1433-1438.

Huang SF, Ding Y, Ruan JW, Zhang W, Wu JL, He B, Zhang YJ, Li Y, Zeng YS (2011) An experimental electro-acupuncture study in treatment of the rat demyelinated spinal cord injury induced by ethidium bromide. Neurosci Res 70:294-304.

Joshi M, Fehlings MG (2002) Development and characterization of a novel, graded model of clip compressive spinal cord injury in the mouse: Part 1. Clip design, behavioral outcomes, and histopathology. J Neurotrauma 19:175-190.

Karsan A (2005) The role of notch in modeling and maintaining the vasculature. Can J Physiol Pharmacol 83:14-23.

Li WJ, Pan SQ, Zeng YS, Su BG, Li SM, Ding Y, Li Y, Ruan JW (2010) Identification of acupuncture-specific proteins in the process of electro-acupuncture after spinal cord injury. Neurosci Res 67:307-316.

Liu ZJ, Shirakawa T, Li Y, Soma A, Oka M, Dotto GP, Fairman RM, Velazquez OC, Herlyn M (2003) Regulation of Notch1 and Dll4 by vascular endothelial growth factor in arterial endothelial cells: implications for modulating arteriogenesis and angiogenesis. Mol Cell Biol 23:14-25.

Livak KJ, Schmittgen TD (2001) Analysis of relative gene expression data using real-time quantitative PCR and the 2(-Delta Delta C(T)) Method. Methods 25:402-408.

Louvi A, Artavanis-Tsakonas S (2006) Notch signalling in vertebrate neural development. Nat Rev Neurosci 7:93-102.

Loy DN, Crawford CH, Darnall JB, Burke DA, Onifer SM, Whittemore SR (2002) Temporal progression of angiogenesis and basal lamina deposition after contusive spinal cord injury in the adult rat. J Comp Neurol 445:308-324.

Mekhail M, Almazan G, Tabrizian M (2012) Oligodendrocyte-protection and remyelination post-spinal cord injuries: a review. Prog Neurobiol 96:322-339.

Morshead CM, Reynolds BA, Craig CG, McBurney MW, Staines WA, Morassutti D, Weiss S, van der Kooy D (1994) Neural stem cells in the adult mammalian forebrain: a relatively quiescent subpopulation of subependymal cells. Neuron 13:1071-1082.

Munce SE, Perrier L, Tricco AC, Straus SE, Fehlings MG, Kastner M, Jang E, Webster F, Jaglal SB (2013) Impact of quality improvement strategies on the quality of life and well-being of individuals with spinal cord injury: a systematic review protocol. Syst Rev 2:14.

Ohri SS, Maddie MA, Zhao Y, Qiu MS, Hetman M, Whittemore SR (2011) Attenuating the endoplasmic reticulum stress response improves functional recovery after spinal cord injury. Glia 59:1489-1502.

Parent JM, Vexler ZS, Gong C, Derugin N, Ferriero DM (2002) Rat forebrain neurogenesis and striatal neuron replacement after focal stroke. Ann Neurol 52:802-813.

Park E, Velumian AA, Fehlings MG (2004) The role of excitotoxicity in secondary mechanisms of spinal cord injury: a review with an emphasis on the implications for white matter degeneration. J Neurotrauma 21:754-774.

Pineau I, Lacroix S (2007) Proinflammatory cytokine synthesis in the injured mouse spinal cord: multiphasic expression pattern and identification of the cell types involved. J Comp Neurol 500:267-285.

Poon PC, Gupta D, Shoichet MS, Tator CH (2007) Clip compression model is useful for thoracic spinal cord injuries: histologic and functional correlates. Spine (Phila Pa 1976) 32:2853-2859.

Qin W, Bauman WA, Cardozo C (2010) Bone and muscle loss after spinal cord injury: organ interactions. Ann N Y Acad Sci 1211:66-84.

Rice T, Larsen J, Rivest S, Yong VW (2007) Characterization of the early neuroinflammation after spinal cord injury in mice. J Neuropathol Exp Neurol 66:184-195.

Su Z, Yuan Y, Chen J, Zhu Y, Qiu Y, Zhu F, Huang A, He C (2011) Reactive astrocytes inhibit the survival and differentiation of oligodendrocyte precursor cells by secreted TNF-alpha. J Neurotrauma 28:1089-1100.

Suh H, Consiglio A, Ray J, Sawai T, D'Amour KA, Gage FH (2007) In vivo fate analysis reveals the multipotent and self-renewal capacities of Sox2+ neural stem cells in the adult hippocampus. Cell Stem Cell 1:515-528.

Sun F, Lin CL, McTigue D, Shan X, Tovar CA, Bresnahan JC, Beattie MS (2010) Effects of axon degeneration on oligodendrocyte lineage cells: dorsal rhizotomy evokes a repair response while axon degeneration rostral to spinal contusion induces both repair and apoptosis. Glia 58:1304-1319.

Trivedi A, Olivas AD, Noble-Haeusslein LJ (2006) Inflammation and Spinal Cord Injury: Infiltrating Leukocytes as Determinants of Injury and Repair Processes. Clin Neurosci Res 6:283-292.

Zhao C, Deng W, Gage FH (2008) Mechanisms and functional implications of adult neurogenesis. Cell 132:645-660.